

HYBRID ELECTRIC VEHICLES

UNIT-4

Sl.no	List of contents	Page number
1	Boost and Buck-Boost converters	2-5
2	Multi Quadrant DC-DC converters	8 - 13
3	DC-AC Inverter for EV and HEV applications	14
4	Three Phase DC-AC inverters - Voltage control of DC-AC inverters using PWM	15-19
5	EV and PHEV battery chargers.	19-23

1.Boost and Buck-Boost converters:

4.1.2 STEADY-STATE OPERATION OF SWITCH-MODE DC-DC CONVERTER

In switch-mode dc–dc converter, the term “switch” comes from the fact that the converter comprises at least one switching device. This device is a semiconductor component enabling the circulation (on state) or not (off state) of a current through it. The state (on and off) of the semiconductor is either defined by the electric circuit (e.g., diode) or controlled by a periodic gate signal u , which is characterized by its duty cycle d over a period T (e.g., MOSFET and IGBT). The value of d represents the average value of u over the period T , as represented in Figure 4.1. The steady-state operation of a dc–dc converter corresponds to the expression of the input/output currents and voltages according to d . It specifies the root mean square (RMS) output voltage of the converter according to the RMS input voltage and the duty cycle. In the section presented here, it is assumed that all the converters operate in continuous conduction mode (CCM). This means that the current within the inductor is always higher than 0.

4.1.2.1 Buck Converter

An electrical circuit of the Buck converter with ideal switches is represented in Figure 4.2. The Buck converter enables to step down the input voltage. When S_1 is on, $V_L = V_{in} - V_{out}$, and when S_1 is off, $V_L = -V_{out}$. Over a period of time, the average value of V_L is null in the steady state. If not, it means that the steady state is not reached yet. Hence, relation (4.1) can be expressed to obtain the transformation ratio between V_{in} and V_{out} . Considering Equation 4.1, the transformation ratio between V_{in} and V_{out} in the steady state is given by relation (4.2), where d is the duty cycle of S_1 .

$$V_L = \frac{1}{T} \left(\int_0^{dT} V_{in} - V_{out} dt + \int_{dT}^T -V_{out} dt \right) = 0 \quad (4.1)$$

$$\Rightarrow d \cdot V_{in} = V_{out} \quad (4.2)$$

As the duty cycle is comprised between 0 (S_1 always open) and 1 (S_1 always closed), V_{out} has a value ranging between 0 and V_{in} .

If we consider that all the components are perfect, there is no loss within the converter, and the input power (4.3) is equal to the output power (4.4) in the steady state. Then, by considering Equations 4.2, 4.4, and 4.5, the relation between the input current and the output current can be expressed as Equation 4.6.

$$P_{in} = V_{in} \cdot i_{in}, \quad (4.3)$$

$$P_{out} = V_{out} \cdot i_{out} \quad (4.4)$$

$$P_{in} = P_{out} \quad (4.5)$$

$$\Rightarrow d \cdot i_{out} = i_{in} \quad (4.6)$$

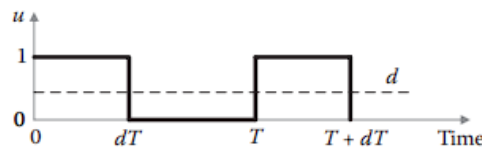


FIGURE 4.1 Gate signal u .

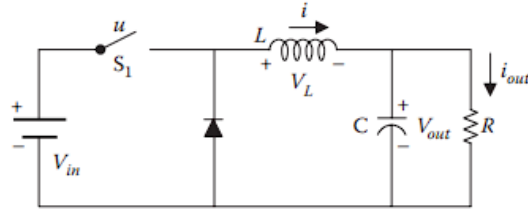


FIGURE 4.2 Buck converter.

4.1.2.2 Boost Converter

Boost converter steps up the input voltage. Considering ideal switches, its electrical circuit is represented in Figure 4.3. When S_1 is on, the diode is reverse biased and the inductor L is charged by the source (V_{in}) and $V_L = V_{in}$. Then, when S_1 is off, energy stored within the inductance is transmitted to the dc-link capacitor and $V_L = V_{in} - V_{out}$. This energy transfer yields the generation of an output voltage higher than the input voltage. In an electrified vehicle, such a converter can be used between the battery pack and the traction inverter. This is the case in the Toyota Prius 2010.

Over an entire period, the average value of V_L is equal to 0 in a steady-state operation. Hence, relation (4.7) can be expressed to obtain the transformation ratio between V_{in} and V_{out} . The steady-state relation between V_{in} and V_{out} is given by relation (4.8), where d is the duty cycle of S_1 .

$$V_L = \frac{1}{T} \left(\int_0^{dT} V_{in} dt + \int_{dT}^T V_{in} - V_{out} dt \right) = 0 \quad (4.7)$$

$$\Rightarrow V_{in} = (1 - d) \cdot V_{out} \quad (4.8)$$

As was done for the Buck converter, relations (4.3) through (4.5) and (4.8) can be used to express Equation 4.9 that expresses the current levels of Boost converter in the steady state.

$$i_{out} = (1 - d) \cdot i_{in} \quad (4.9)$$

In the ideal case, Equation 4.8 shows that V_{out} can be theoretically boosted up to infinity (case $d = 1$). However, an infinite output voltage is obviously not possible in practice. Indeed, parasitic resistive elements of the circuit limit the maximum output voltage reachable by the converter. For instance, if the series resistance r_L of the inductor windings is considered, the steady-state relation becomes Equation 4.10.

$$V_{in} = \left(1 - d + \frac{r_L}{R \cdot (1 - d)} \right) \cdot V_{out} \quad (4.10)$$

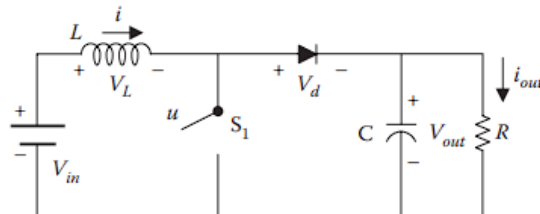


FIGURE 4.3 Boost converter.

4.1.2.3 Buck–Boost Converter

Buck–Boost converter enables to either step up or step down the output voltage. Considering an ideal switch, its electrical topology is given in Figure 4.4. The switch S_1 permits to store energy within the inductor. When S_1 is “on-state,” the voltage across the inductor is $V_L = V_{in}$, and the current is circulating from the input voltage source to the inductor. Then, when S_1 is “off-state,” the energy stored within the inductor is transmitted to the dc-link capacitor through the diode. During this phase, $V_L = -V_{out}$. In steady-state operation, over one period, as explained above, the average value of V_L is zero, and hence relation (4.11) can be expressed to obtain the transformation ratio between V_{in} and V_{out} . From Equation 4.12, it can be seen that if $d < 0.5$, then $V_{out} < V_{in}$ and the converter operates in the Buck mode. Inversely, if $d > 0.5$, then $V_{out} > V_{in}$ and the converter operates in the Boost mode.

$$V_L = \frac{1}{T} \left(\int_0^T V_{in} dt + \int_{dT}^T -V_{out} dt \right) = 0 \quad (4.11)$$

$$\Rightarrow V_{in} \cdot d = (1 - d) \cdot V_{out} \quad (4.12)$$

Similarly, for the Buck and Boost converters, if the converter is considered as ideal, and hence without any loss, Equations 4.3 through 4.5 and 4.12 can be considered to express Equation 4.13.

$$i_{out} \cdot d = (1 - d) \cdot i_{in} \quad (4.13)$$

From Equation 4.12, it can be seen that the ideal Buck–Boost converter can theoretically generate an infinite output voltage (case $d = 1$). As it has been mentioned for the Boost converter, this is not achievable in practice due to the parasitic resistivity of the components. Indeed, considering the series resistance r_L of the inductor, Equation 4.12 becomes Equation 4.14.

$$d \cdot V_{in} = \left(1 - d + \frac{r_L}{R \cdot (1 - d)} \right) \cdot V_{out} \quad (4.14)$$

4.1.2.4 Summary of Steady-State Characteristics of Presented dc–dc Converters

In Figure 4.5, the steady-state characteristics of each converter are plotted, which are given by Equation 4.1 for the Buck, Equations 4.8 and 4.10 for the Boost, and Equations 4.12 and 4.14 for the Buck–Boost. When selecting a topology, the designer should keep in mind that the more the duty cycle, the less the efficiency. This point is more detailed in Section 4.3.2.3. Thus, even if a Boost or a Buck–Boost offers theoretically very high step-up capabilities, they are limited in practice because of a too low efficiency in these operating areas.

4.1.3 OVERVIEW OF SWITCHING DEVICES

In the previous section, steady-state operations of three different dc–dc converters were presented. As it has been mentioned, these converters operate by way of semiconductors. Owing to their

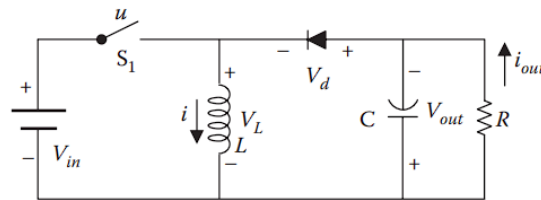


FIGURE 4.4 Buck–Boost converter.

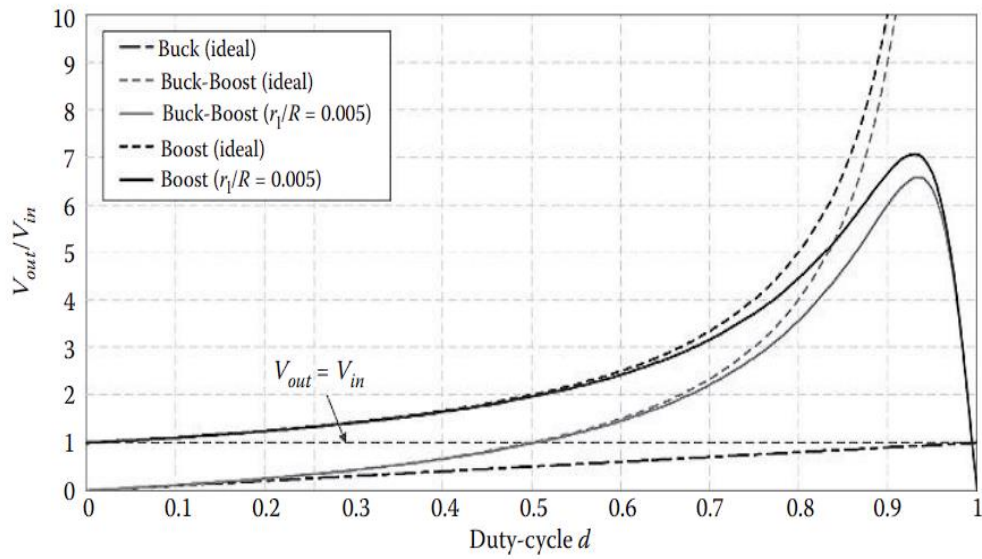


FIGURE 4.5 Steady-state characteristics of the Buck, Buck–Boost, and Boost converters.

complexity, semiconductors are very often considered as ideal in power electronics circuit analysis. This approach simplifies a lot the analysis of the circuit and lets the designer focus on the electrical operation of the converter instead of the semiconductor itself. Nevertheless, it is important to have an understanding of how to select a semiconductor for an application as the use of an inappropriate device reduces the good operation of the converter and often leads to its failure. First, this section proposes an overview of the electrical characteristics of a switch, and then presents ideal characteristics of most used semiconductors in power electronics design. More detailed information about nonideal characteristics and properties of semiconductor devices can be found in References 3,4.

POWER CONVERTERS

The power converter can be a DC drive supplying a DC motor or an AC drive supplying an AC motor. The converter functions of the two types of drives are shown in [Figure 7.2](#). The power electronic drive requirement for switched reluctance (SR) machines is different from that of DC or AC drives and, hence, will be discussed separately in [Chapter 8](#).

A power converter is made of high-power fast-acting semiconductor devices, such as bipolar junction transistor (BJT), metal oxide semiconductor field effect transistor (MOSFET), insulated gate bipolar transistor (IGBT), silicon-controlled rectifier or thyristor (SCR), gate turn-off SCR (GTO), and MOS-controlled

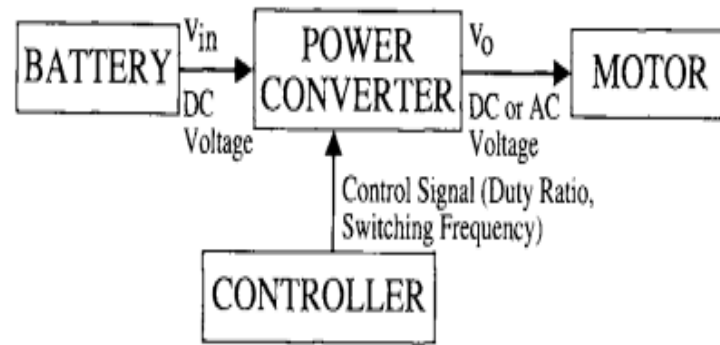


FIGURE 7.1 Block diagram of a motor drive.

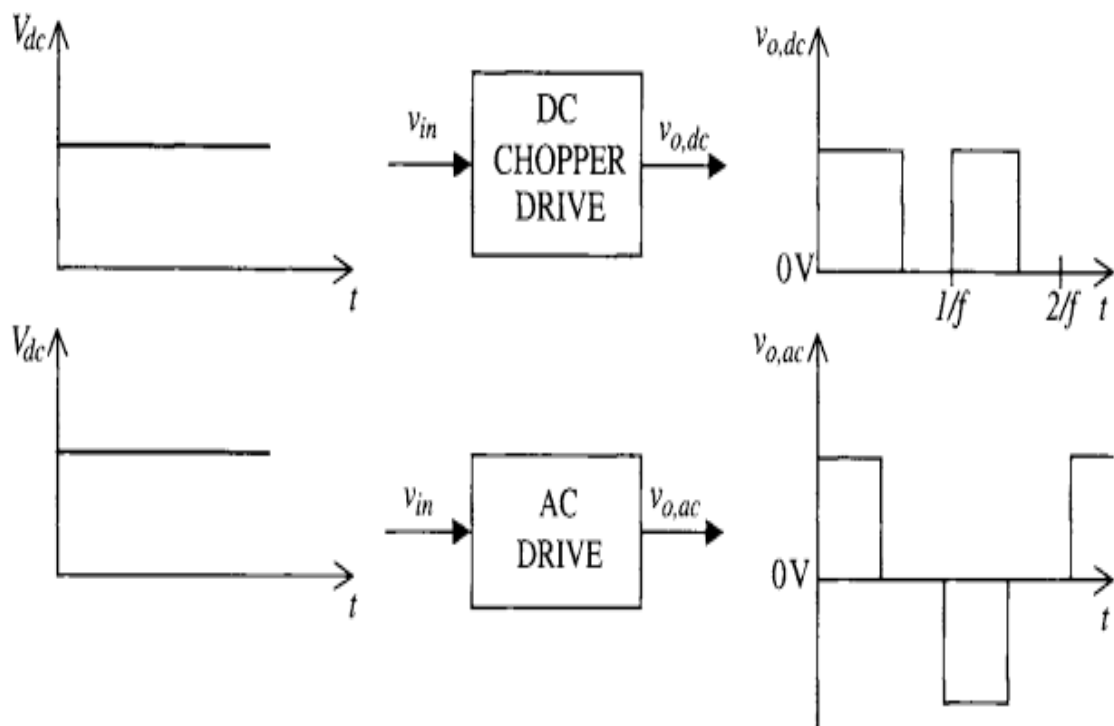


FIGURE 7.2 DC-DC and DC-AC converter functions.

thyristor (MCT). These solid-state devices configured in a certain circuit topology function as an on-off electronic switch to convert the fixed supply voltage into variable voltage and variable frequency supply. All of these devices have a control input gate or base through which the devices are turned on and off according to the command generated by the controller. Tremendous advances in power semiconductor technology over the past two decades enabled the development of compact, efficient, and reliable DC-DC and DC-AC power electronic converter topologies.

2. Multi Quadrant DC-DC converters:

DC DRIVES

The DC drives for EV and HEV applications are the DC-DC converters, such as DC-choppers, resonant converters, or push-pull converters. A two-quadrant chopper will be analyzed in this chapter as representative of DC drives. The simplicity of the two-quadrant chopper and the torque-speed characteristics of the separately excited DC motor will be utilized to present the interaction of a

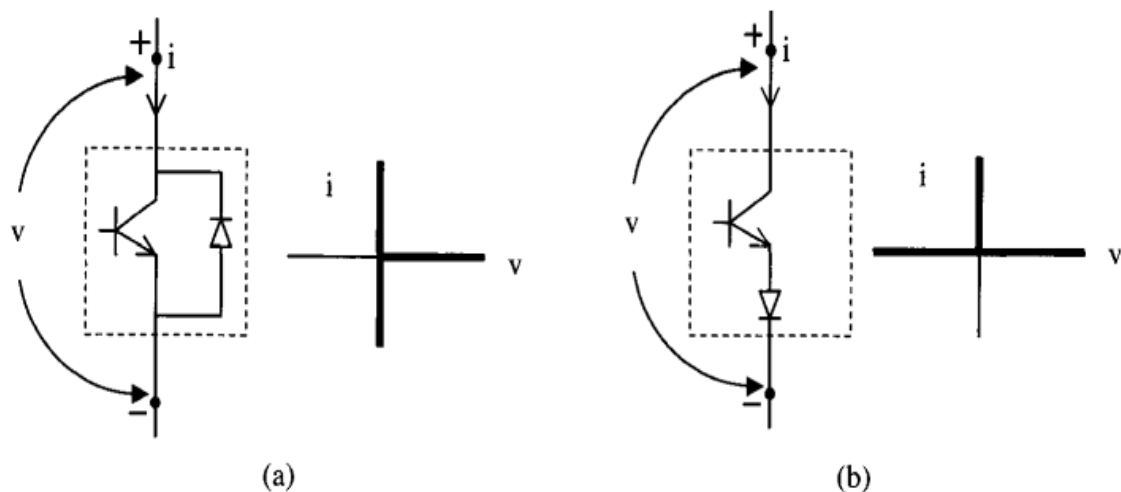


FIGURE 7.7 (a) Bidirectional current switch. (b) Bidirectional voltage switch.

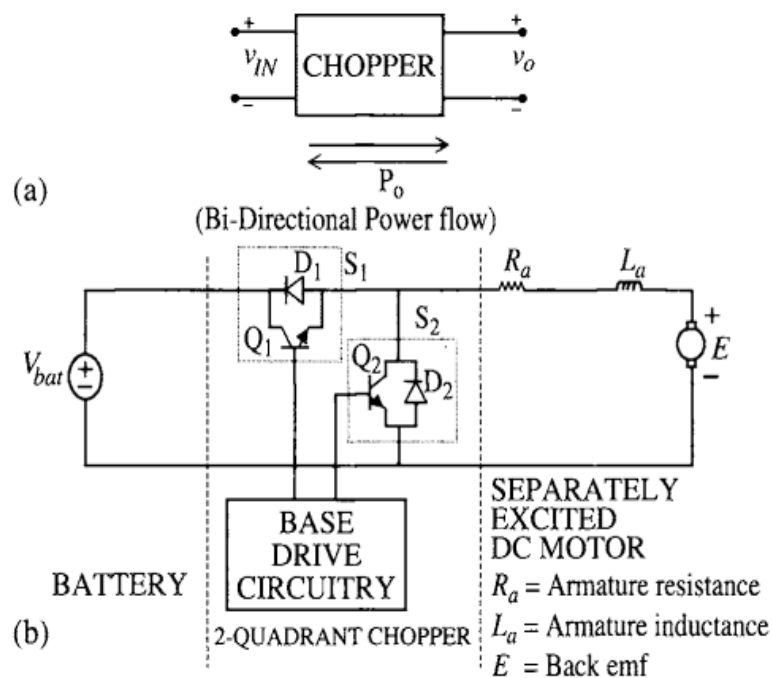


FIGURE 7.8 A DC motor drive. (a) Power flow in drive; (b) drive circuit.

TWO-QUADRANT CHOPPER

The two-quadrant DC chopper allows bidirectional current and power flow with unidirectional voltage supply. The schematic of a two-quadrant chopper is shown in Figure 7.8. The motor current i_o is inductive current and, therefore, cannot change instantaneously. The transistor Q_1 and diode D_1 combined make the bidirectional current switch S_1 . Similarly, switch S_2 is made of transistor Q_2 and diode D_2 . The on and off conditions of the two switches make four switching

states (SWS), two of which are allowed and two are restricted, as shown in Table 7.2. In the allowed switching states SWS1 and SWS2, the switches S_1 and S_2 have to withstand positive voltage when they are off and both positive and negative currents when they are on. Therefore, bidirectional current switches have been used.

TABLE 7.2 Switching States of Two-Quadrant Chopper

Switching State	S_1	S_2	Comments
SWS 0	0 (OFF)	0 (OFF)	Not applicable in CCM, because i_o is inductive
SWS 1	0	1 (ON)	$v_o = 0$; $v_{S1} = v_{IN}$ (allowed) $i_{IN} = 0$; $i_{S2} = -i_o$
SWS 2	1	0	$v_o = v_{IN}$; $v_{S2} = v_{IN}$ (allowed) $i_{IN} = i_o$; $i_{S1} = i_o$
SWS 3	1	1	Not allowed, because v_{IN} will get shorted

In Quadrant I operation, turning on Q_1 allows current and power to flow from the battery to the motor. Motor terminal voltage v_o and current i_o are greater than or equal to zero. Q_2 is required to remain continuously off in Quadrant I operation and, hence, $i_{b2}=0$. When Q_1 turns off, D_2 turns on, because i_o is continuous. Quadrant I operation takes place during the acceleration and constant velocity cruising of a vehicle. The chopper operating modes toggle between switching states 1 and 2 in this quadrant, as shown in Figure 7.9.

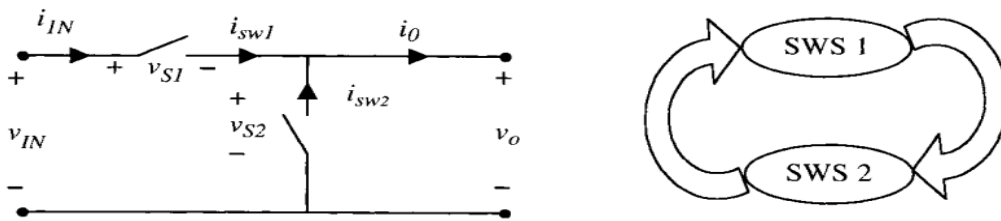


FIGURE 7.9 Quadrant I operation.

The transistor Q_1 switches at fixed chopper frequency to maintain the desired current and torque output of the DC motor. The motor current i_o was shown in Figure 7.10 with exaggerated ripple, where in practice, the ripple magnitude is much smaller compared to the average value of i_o . The filtering requirements set the time period of switching such that a smooth current and torque output is available. The output of the outer-loop vehicle controller desiring a specific torque output of the motor is the duty-ratio d , which sets the on-time of the transistor Q_1 . d is a number between 0 and 1, which when multiplied by the time period T , gives the on-time of the transistor. The gate drive signal for Q_1 is a function of d , and consequently, assuming ideal switching conditions, the input

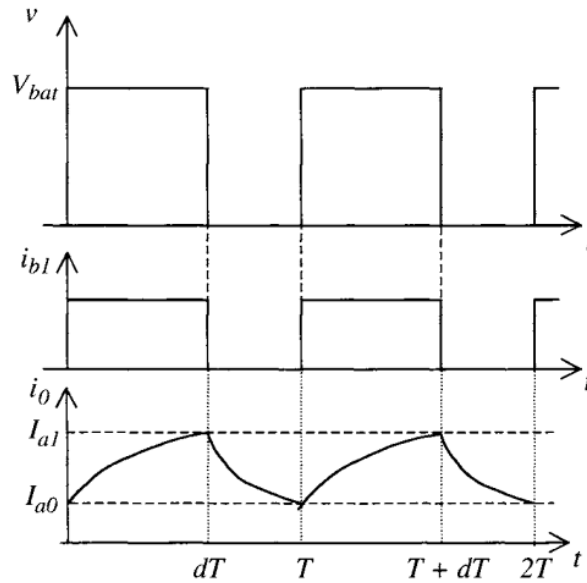


FIGURE 7.10 Output voltage, gate drive for Q_1 , and motor current.

voltage to the motor is also dependent on d . The circuit configurations in the two allowed switching states are shown in [Figure 7.11](#) to aid the steady state analysis of the drive system. The steady state analysis is carried out assuming the ideal conditions that there are no switching losses and no delay in the turn-on and turn-off of the devices.

OPEN-LOOP DRIVE

From a systems perspective, the two-quadrant chopper drives the DC motor that delivers power to the transmission and wheels for vehicle propulsion, as shown in [Figure 7.12](#). Input to the system comes from the driver of the vehicle through the acceleration pedal and the brake pedal ([Figure 7.13](#)). Acceleration and constant speed cruising are controlled by Q_1 in Quadrant I operation, while braking is controlled by Q_2 in Quadrant II operation. In a simplified vehicle control strategy, the slope of the acceleration pedal dictates the desired vehicle motion, and the angle of the pedal is proportionately used to set the duty ratio d_1 for Q_1 . Similarly, the slope of the brake pedal expresses the amount of braking desired, and the angle of the brake pedal is proportionately used to set the duty ratio d_2 for Q_2 . The two pedals must not be depressed simultaneously.

As mentioned in [Chapter 5](#), one of the advantages of using electric motors for vehicle propulsion is to save energy during vehicle braking through regeneration. The energy from the wheels is processed by the power converter and delivered to the battery or other energy storage system during regenerative braking. For the two-quadrant chopper, the amount of regeneration per cycle is a function of the duty ratio, as will be shown later. Therefore, the real duty ratio commands of an EV or HEV will be nonlinearly related to the pedal angle, which

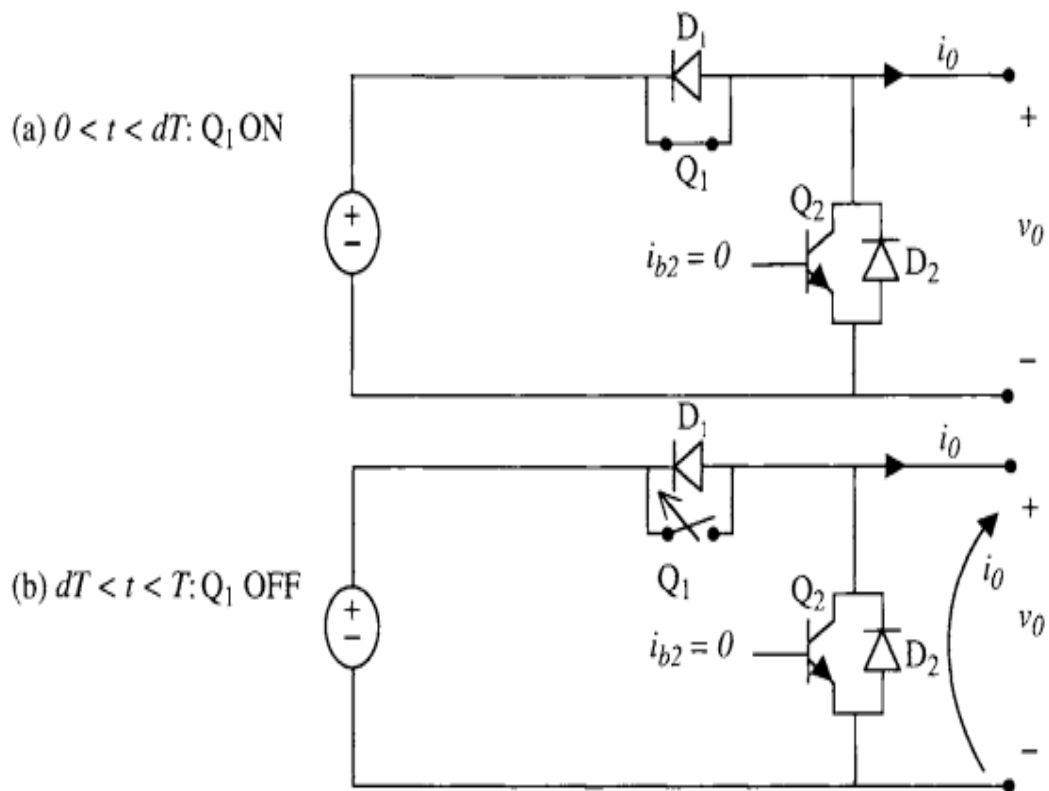


FIGURE 7.11 Circuit condition for (a) switch Q_1 on and (b) for switch Q_2 off.

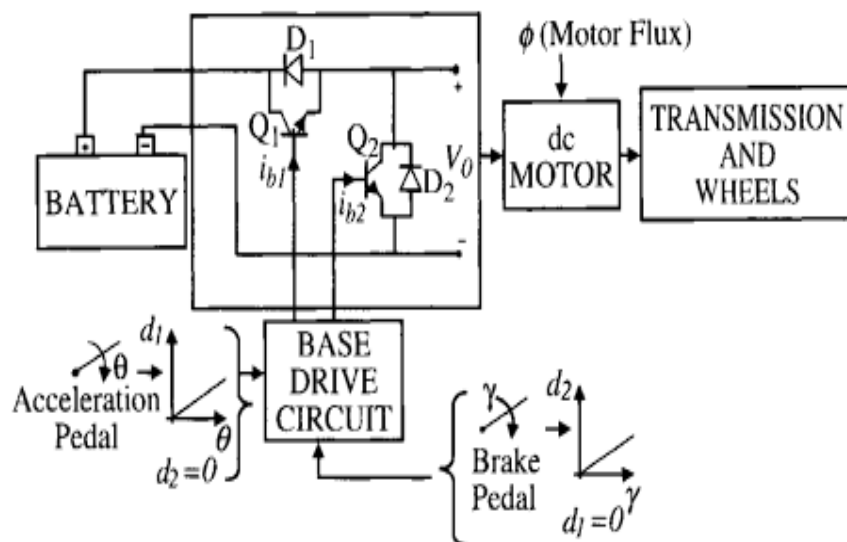


FIGURE 7.12 Open-loop drive for bidirectional power flow.

is assumed in the simplified analysis to follow. However, the simplistic assumption will give good insight into system control.

OPERATING POINT ANALYSIS

The following discussion presents the steady state operating point analysis of the vehicle system at the intersection of the motor torque-speed characteristics with the road load characteristics. Four operating points are chosen for analysis in three different quadrants of the motor speed-torque plane representing four chopper operating modes discussed earlier. These modes are acceleration CCM in Quadrant I ([Scenario 1](#)), acceleration CCM in Quadrant IV ([Scenario 2](#)), acceleration UNCM in Quadrant II ([Scenario 3](#)), and braking CCM in Quadrant II ([Scenario 4](#)). The four scenarios are shown in [Figure 7.24](#).

Now, recall the tractive force vs. vehicle speed characteristics of [Chapter 2](#), which essentially define the speed-torque characteristics of the EV or HEV load. The tractive force vs. velocity characteristics of [Figure 2.11](#) can be converted into equivalent vehicle load speed-torque characteristics, knowing the transmission gear ratio and the vehicle wheel radius. The steady-state operating point of the vehicle for certain conditions of the motor drive system and road load characteristics can be obtained by overlaying the two speed-torque characteristics on the same plot. The steady-state operating points at the intersection of the motor and load characteristics are shown in [Figure 7.25](#).

7.4.1 SCENARIO 1

In this scenario, the vehicle is moving forward on a level roadway with a constant velocity. The chopper is in the acceleration CCM of operation.

7.4.2 SCENARIO 2

The chopper is operating in the acceleration CCM, yet the vehicle is moving backward on a steep uphill road. If the duty ratio has not yet reached 100%, d_1 can be increased all the way up to 1 by depressing the acceleration pedal further and increasing the torque output of the motor. Increasing d_1 will raise the motor speed-torque characteristics vertically upwards, enabling a possible steady state

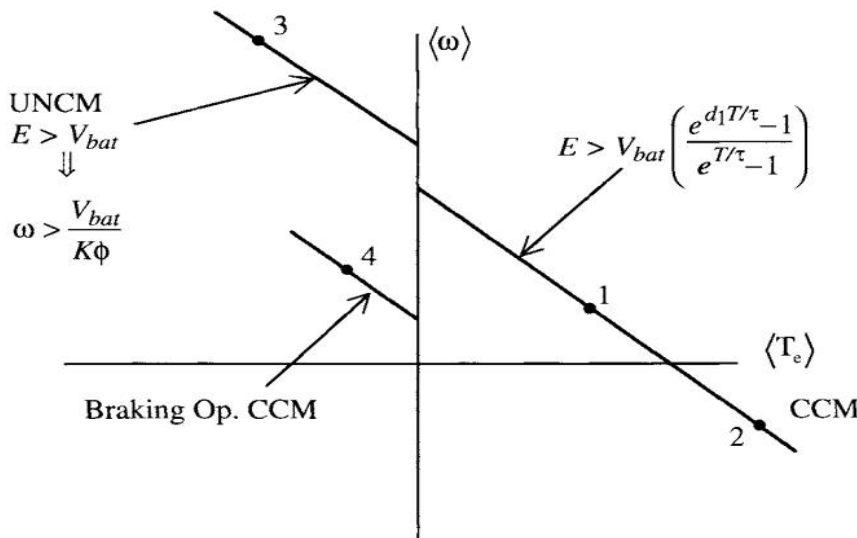


FIGURE 7.24 Motor speed-torque characteristics for four chopper modes.

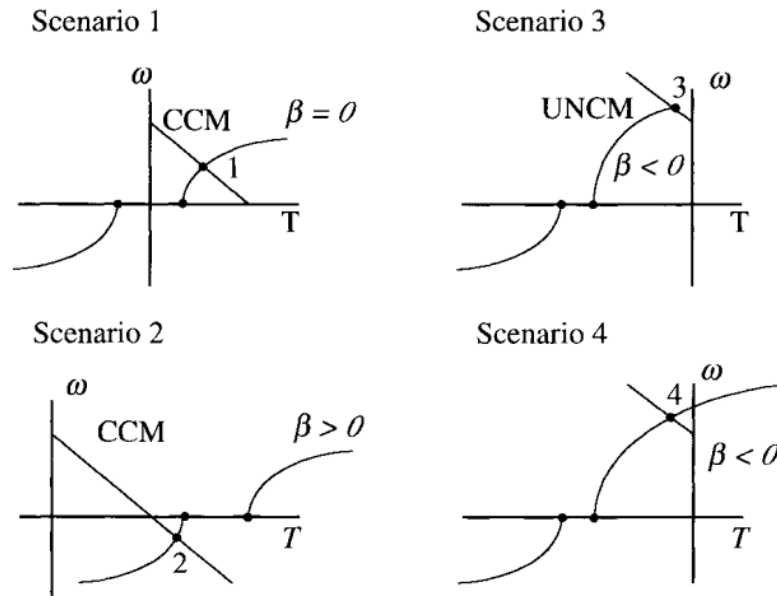


FIGURE 7.25 Operating point analysis for the scenarios.

operating point in the first quadrant. If the motor rating has reached its limit, then the torque cannot be increased further to overcome the road load resistance. The slope is too steep for the rating of the motor, and the vehicle rolls backward. The wheel back-drives the motor in this case.

7.4.3 SCENARIO 3

The vehicle is going downhill, with the chopper operating in the acceleration mode. The angle of the acceleration pedal will have no bearing on the steady state operating point. There will be uncontrolled regeneration into the energy source.

7.4.4 SCENARIO 4

The vehicle is going downhill in a controlled fashion using the brake pedal. The speed of the vehicle going down the slope is in the control of the driver.

3.DC-AC Inverter for EV and HEV applications:

The voltage source inverter, shown in Figure 8.1, is common for EV and HEV applications, where the source typically delivers a stiff voltage. The six-switch voltage source inverter can operate in the six-step mode or in the pulse width modulation (PWM) mode. The inverter output invariably has a number of harmonic components in addition to the desired fundamental voltage component. PWM is used to minimize the harmonic contents of the output voltage signal. There are several methods of generating PWM signals, such as, sinusoidal PWM, state vector PWM, uniform sampling PWM, selective harmonic elimination, etc. The electronic controller generates the gate switch signals for the inverter power devices using a PWM method and control commands to process the power flow and deliver the output voltage at desired voltage and frequency. Six-switch inverter topology is used for induction machines as well as for permanent magnet (PM) or any other synchronous machines

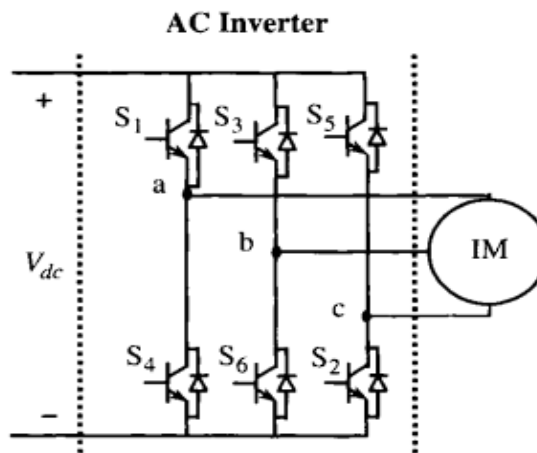


FIGURE 8.1 Six-switch voltage source inverter.

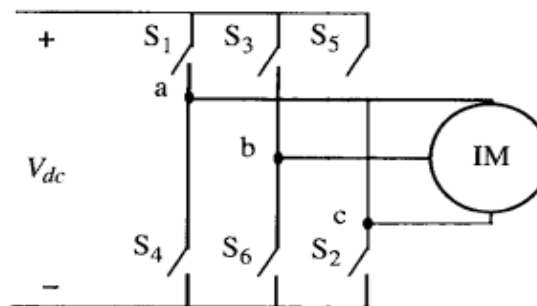


FIGURE 8.2 Ideal six-switch voltage source inverter.

can be achieved from a scalar control method; hence, vector control methods based on the reference frame transformation theory are used. Vector control is characterized by involving magnitude and phase control of the applied voltage. Control algorithms are much more complex and computationally intensive for vector control methods. Computational burden is greatly alleviated through the advances of microprocessor and digital signal processor technology. The vector control technique is a well-developed technology with several drive manufacturing companies offering products for various industrial applications.

4.Three Phase DC-AC inverters:

4.2.2 THREE-PHASE INVERTER

Three-phase inverters are used to transform a dc-voltage source into a three-phase ac output. The two main applications of this type of inverter are: high-power grid-tie inverter for electrical energy transportation and three-phase ac drive system. Three-phase ac drive system is very important in any transportation application as almost every motor used for traction (automotive, railway, ship) are three-phase ac.

4.2.2.1 Electrical Circuit

Electrical circuit of a three-phase inverter is presented in Figure 4.39. It is composed of three legs in parallel to the dc voltage source. The middle point of each leg corresponds to one of the three outputs of the converter. In motor drive application, the three phases of the motor are connected in Y configuration, and are connected to the middle point of each leg, as in Figure 4.39. Three-phase inverter is composed of six bidirectional switches, such as MOSFET or IGBT with an antiparallel diode. Electrical characteristics of the switches are the same as for the single-phase configuration. Also, similar to that for the single-phase inverter, the two switches of one leg cannot be closed simultaneously. If this happens, the dc-voltage source is short-circuited.

4.2.2.2 Line-to-Line and Phase Voltages

Considering electrical configuration of Figure 4.39, the line-to-line and phase voltages of the inverter's load can be expressed according to the gate signal of the switches and the dc-bus voltage. In Table 4.5, the different line-to-line voltage possibilities are given.

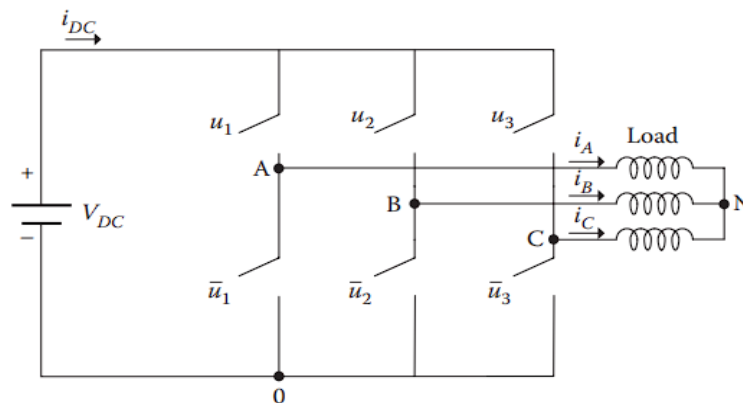


FIGURE 4.39 Electrical circuit of three-phase inverter.

TABLE 4.5
Line-to-Line Voltage

u_1	u_2	u_3	V_{AB}	V_{BC}	V_{CA}
1	1	0	0	V_{dc}	$-V_{dc}$
1	0	1	V_{dc}	$-V_{dc}$	0
0	1	1	$-V_{dc}$	0	V_{dc}
0	0	1	0	$-V_{dc}$	V_{dc}
0	1	0	$-V_{dc}$	V_{dc}	0
1	0	0	V_{dc}	0	$-V_{dc}$
1	1	1	0	0	0
0	0	0	0	0	0

TABLE 4.6
Line-to-Neutral Voltage

u_1	u_2	u_3	V_{A0}	V_{B0}	V_{C0}
1	1	0	V_{dc}	V_{dc}	0
1	0	1	V_{dc}	0	V_{dc}
0	1	1	0	V_{dc}	V_{dc}
0	0	1	0	0	V_{dc}
0	1	0	0	V_{dc}	0
1	0	0	V_{dc}	0	0
1	1	1	0	0	0
0	0	0	V_{dc}	V_{dc}	V_{dc}

In Table 4.6, the line-to-neutral voltages are given. These voltages can be easily obtained from the electrical circuit of the inverter. In an opposite way, phase voltages of the load are not obvious to determine from the electrical circuit. Nevertheless, it can be demonstrated that they are linked to the line-to-neutral voltage by relation (4.53). Obtained phase voltages are expressed in Table 4.7. It can be noticed that the maximum voltage that can be applied to a phase of the load is equal to $|2/3 \times V_{dc}|$.

$$\begin{bmatrix} V_{AN} \\ V_{BN} \\ V_{CN} \end{bmatrix} = \frac{1}{3} \begin{bmatrix} 2 & -1 & -1 \\ -1 & 2 & -1 \\ -1 & -1 & 2 \end{bmatrix} \begin{bmatrix} V_{A0} \\ V_{B0} \\ V_{C0} \end{bmatrix} \quad (4.53)$$

4.2.2.3 dc-Side Current

The dc-side current of a three-phase inverter is expressed by Equation 4.54. Considering relation (4.55), which corresponds to the Y configuration of the load, and relation (4.53), dc-side currents corresponding to each state configuration of the inverter are expressed in Table 4.8.

$$i_{DC} = u_1 \times i_A + u_2 \times i_B + u_3 \times i_C \quad (4.54)$$

$$0 = i_A + i_B + i_C \quad (4.55)$$

4.2.2.4 PWM in Three-Phase Inverter

The principal function of a three-phase inverter is to generate a three-phase ac output from a dc input. In motor drive application, the frequency of the output, as well as its amplitude, is used to control the speed and torque of the motor. To generate both frequency-and amplitude-variable outputs, a

TABLE 4.7
Phase Voltage

u_1	u_2	u_3	V_{AN}	V_{BN}	V_{CN}
1	1	0	$1/3 \times V_{dc}$	$1/3 \times V_{dc}$	$-2/3 \times V_{dc}$
1	0	1	$1/3 \times V_{dc}$	$-2/3 \times V_{dc}$	$1/3 \times V_{dc}$
0	1	1	$-2/3 \times V_{dc}$	$1/3 \times V_{dc}$	$1/3 \times V_{dc}$
0	0	1	$-1/3 \times V_{dc}$	$-1/3 \times V_{dc}$	$2/3 \times V_{dc}$
0	1	0	$-1/3 \times V_{dc}$	$2/3 \times V_{dc}$	$-1/3 \times V_{dc}$
1	0	0	$2/3 \times V_{dc}$	$-1/3 \times V_{dc}$	$-1/3 \times V_{dc}$
1	1	1	0	0	0
0	0	0	0	0	0

TABLE 4.8
dc-Side Current

u_1	u_2	u_3	i_{DC}
1	1	0	$-i_C$
1	0	1	$-i_B$
0	1	1	$-i_A$
0	0	1	i_C
0	1	0	i_B
1	0	0	i_A

three-phase PWM scheme can be used, as represented in Figure 4.40. As was detailed in the previous section, when using a sinusoidal reference, the generated output has its fundamental at the frequency of the reference signal, and its amplitude is proportional to the modulation index (defined as the ratio between the reference signal's amplitude and the carrier's amplitude). Considering signals defined in Figure 4.40, RMS values of the load's phase voltage is given by Equation 4.56.

$$V_{phase\ rms} = \frac{V_m}{\sqrt{2}} \times \frac{V_{DC}}{2} \quad (4.56)$$

In Figure 4.41, line-to-line and phase voltages obtained using the PWM scheme of Figure 4.40 are plotted. It can be seen that values of the line-to-line and phase voltage are in accordance with the ones given in Tables 4.5 and 4.7, respectively.

Corresponding dc-side and phase current waveforms are shown in Figure 4.42. The value of the dc-side current is always equal to one of the phase current or its opposite. Relations given in Table 4.8 specify the value of i_{DC} according to the gate signals. The RMS value of the current is given by Equation 4.57, where P is the input power of the inverter.

$$i_{DCrms} = \frac{P}{V_{DC}} \quad (4.57)$$

Current flowing through one of the switches is the one circulating through its corresponding phase when its gate signal is 1 (switch in “on-state”). This state of period and pattern is defined by the duty cycle, and thus by the controller. The duty cycle is not constant; it varies continuously as it follows the PWM.

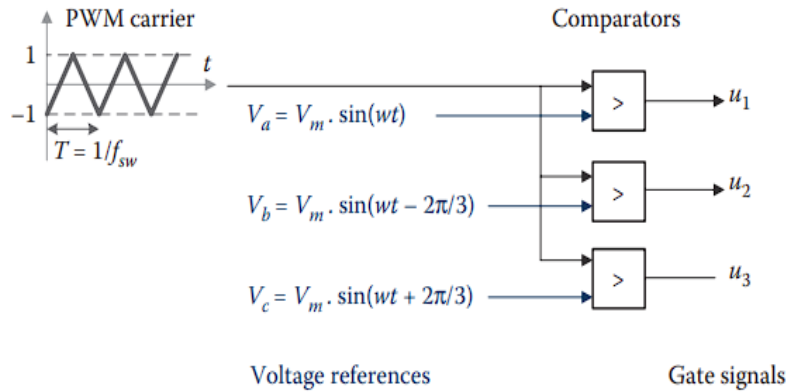


FIGURE 4.40 PWM scheme for three-phase inverter.

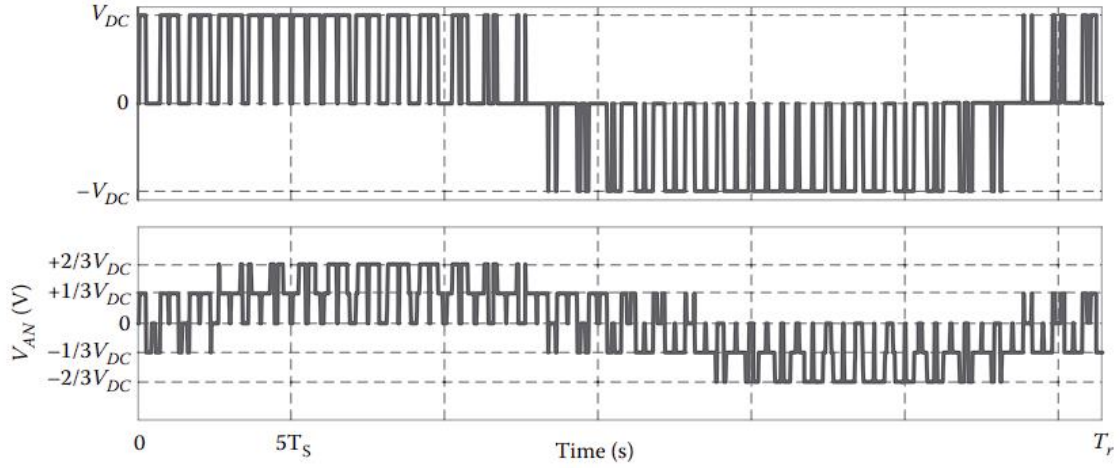


FIGURE 4.41 Line-to-line and phase voltages generated by three-phase inverter and PWM scheme.

4.2.2.5 Output Power of Three-Phase Inverter

If we assume that the phase voltages and current across the load are the one defined in Equations 4.58 and 4.59, respectively, then the true output power (expressed in watts) transmitted to the load by the inverter is given by Equation 4.60, and can be simplified into Equation 4.61. As for the single-inverter case, $\cos(\phi)$ is defined as the power factor of the load, which can be obtained from the load by Equation 4.52. However, in motor drive application, current feedback is used to control the motor and, according to the control algorithm, the power factor of the motor can be changed to improve the efficiency/controllability of the drive system. Conventionally used control method such as space-vector-control enables to keep the angle between the magnetic fields of the rotor and the stator in a way (typically around 90°) to keep the power factor at a high value, and thus to ensure high efficiency of the motor. This is further discussed in Chapter 6.

$$\begin{aligned}
 V_{AN} &= V_{RMS} \sqrt{2} \cos(\omega t) \\
 V_{BN} &= V_{RMS} \sqrt{2} \cos\left(\omega t - \frac{2\pi}{3}\right) \\
 V_{CN} &= V_{RMS} \sqrt{2} \cos\left(\omega t + \frac{2\pi}{3}\right)
 \end{aligned} \tag{4.58}$$

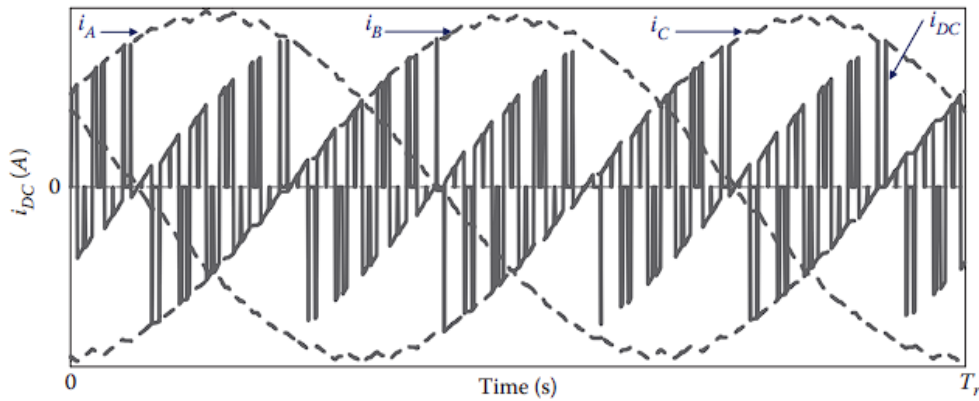


FIGURE 4.42 Phase and dc-side currents generated by three-phase inverter and PWM scheme.

$$i_A = I_{RMS} \sqrt{2} \cos(\omega t + \phi), \quad i_B = I_{RMS} \sqrt{2} \cos\left(\omega t - \frac{2\pi}{3} + \phi\right), \quad i_C = I_{RMS} \sqrt{2} \cos\left(\omega t + \frac{2\pi}{3} + \phi\right) \quad (4.59)$$

$$P = V_{AN}i_A + V_{BN}i_B + V_{CN}i_C \quad (4.60)$$

$$P = 3V_{RMS}I_{RMS}\cos(\phi) \quad (4.61)$$

5.EV and PHEV battery chargers:

13.2 CHARGER CLASSIFICATION AND STANDARDS

A PHEV is a hybrid vehicle with a storage system that can be recharged by connecting a plug to an external electric power source through an AC or DC charging system. The AC charging system is commonly an on-board charger mounted inside the vehicle and is connected to the grid. The DC charging system is commonly an off-board charger mounted at fixed locations, supplying required regulated DC power directly to the batteries inside the vehicle.

13.2.1 AC CHARGING SYSTEMS

The charging AC outlet inevitably needs an on-board AC–DC charger with a power factor correction (PFC). Table 13.1 illustrates charge method electrical ratings according to SAE EV AC charging power levels.

These **chargers** are classified by the level of power they can provide to the battery pack [1]:

- Level 1: Common household circuit, rated up to 120 V AC and up to 16 A. These **chargers** use the standard three-prong household connection, and they are usually considered portable equipment.
- Level 2: Permanently wired electric vehicle supply equipment (EVSE) used especially for electric vehicle charging; rated up to 240 V AC, up to 60 A, and up to 14.4 kW.

TABLE 13.1

Charge Method Electrical Ratings—SAE EV AC Charging Power Levels

Charge Method	Nominal Supply Voltage	Maximum Current	Branch Circuit Breaker Rating	Output Power Level
AC level 1	120 V AC, 1-phase	12 A	15 A	1080 W
	120 V AC, 1-phase	16 A	20 A	1440 W
AC level 2	208–240 V AC, 1-phase	16 A	20 A	3300 W
	208–240 V AC, 1-phase	32 A	40 A	6600 W
	208–240 V AC, 1-phase	≤80 A	Per NEC 635	≤14.4 kW

- Level 3: Permanently wired EVSE used especially for electric vehicle charging; rated greater than 14.4 kW. Fast **chargers** are rated as level 3, but not all level 3 **chargers** are fast **chargers**. This designation depends on the size of the battery pack to be charged and how much time is required to charge the battery pack. A charger can be considered a fast charger if it can charge an average electric vehicle battery pack in 30 min or less.

In summary

- AC **chargers** are commonly on-board the vehicle
 - AC is supplied to the vehicle
 - Charger supplies DC to the battery
 - Must be automotive-grade components
- Considerations for reliability, thermal cycling, vibration, lifetime/warranty, and so on
- High cost to produce and low profit margins for suppliers
- AC levels 1 and 2 are the dominant technologies in production today

13.2.2 DC CHARGING SYSTEMS

The DC charging systems are mounted at fixed locations, like the garage or dedicated charging stations. Built with dedicated wiring, these **chargers** can handle much more power and can charge the batteries more quickly. However, as the output of these **chargers** is DC, each battery system requires the output to be changed for that car. Modern charging stations have a system for identifying the voltage of the battery pack and adjusting accordingly. Table 13.2 illustrates charge method electrical ratings according to SAE EV DC charging power levels.

These **chargers** are classified by the level of power they can provide to the battery pack [1]:

- Level 1: Permanently wired EVSE includes the charger; rated 200–450 V DC, up to 80 A, and up to 36kW

TABLE 13.2

Charge Method Electrical Ratings—SAE EV DC Charging Power Levels

Charge Method	Supplied DC Voltage Range	Maximum Current	Power Level
DC level 1	200–450 V DC	≤80 A DC	≤36 kW
DC level 2	200–450 V DC	≤200 A DC	≤90 kW
DC level 3	200–600 V DC	≤400 A DC	≤240 kW

In summary

- DC **chargers** are off-board (not in the vehicle)
 - AC supplied to a charging box
 - Charger supplies DC to the vehicle
- Consumer-grade components
 - Considerations for reliability, thermal cycling, vibration, and so on not as demanding
 - Lower cost to produce and potentially increased profit margins
- DC level 3 Tesla super**chargers** limited availability
- EVSE includes an off-board charger

13.3 CHARGER REQUIREMENTS

Several considerations and regulatory standards must be met. The charger must comply with the following standards for safety:

- UL 2202: EV Charging System Equipment
- IEC 60950: Safety of Information Technology Equipment
- IEC 61851-21: Electric Vehicle Conductive Charging System—Part 21: Electric Vehicle Requirements for Conductive Connection to an AC–DC Supply
- IEC 61000: Electromagnetic compatibility (EMC)
- ECE R100: Protection against Electric Shock
- ISO 6469-3: Electric Road Vehicles—Safety Specifications—Part 3: Protection of Persons against Electric Hazards
- ISO 26262: Road Vehicles—Functional Safety
- SAE J2929: Electric and Hybrid Vehicle Propulsion Battery System Safety Standard
- FCC Part 15 Class B: The Federal Code of Regulation (CFR) FCC Part 15 for EMC Emission Measurement Services for Information Technology Equipment

In addition, it may be affected by high temperatures, vibration, dust, and other parameters, which comprise the operating environment. Therefore, the charger must meet the following operating environment:

- Engine compartment capable
- IP6K9K, IP6K7 protection class
- –40°C to 105°C ambient air temperature
- –40°C to 70°C liquid coolant temperature

The input and output requirements for a level 2, 3.3 kW charger are also given below.

Input:

- Input voltage range: 85–265 VAC
- Input frequency range: 45–70 Hz
- Input current: 16 ARMS max
- Power factor: ≥ 0.98

Output:

- Output voltage range: 170–440 V DC
- Output power: 3.3 kW max
- Output current: 12 A DC max
- High efficiency: $>94\%$

13.4 TOPOLOGY SELECTION FOR LEVEL 1 AND 2 AC CHARGERS

The front-end AC–DC converter is a key component of the charger system. A variety of circuit topologies and control methods have been developed for the PFC application [2,3]. The single-phase active PFC techniques can be divided into two categories: the single-stage approach and the two-stage approach. The single-stage approach is suitable for low-power applications. In addition, owing to large low-frequency ripple in the output current, only lead acid batteries are chargeable. Furthermore, galvanic isolation is required in on-board battery chargers in order to meet the double fault protection for the safety of the users of PHEV. Therefore, the two-stage approach is the proper candidate for PHEV battery chargers, where the power rating is relatively high, and lithium-ion batteries are used as the main energy storage system. The front-end PFC section is then followed by a DC–DC section to complete the charger system.

Figure 13.1 illustrates a simplified block diagram of a universal input two-stage battery charger used for PHEVs and EVs.

The PFC stage rectifies the input AC voltage and transfers it into a regulated intermediate DC link bus. At the same time, PFC function is achieved. The following DC–DC stage then converts the DC bus voltage into a regulated output DC voltage for charging batteries, which is required to meet the regulation and transient requirements.

13.4.1 FRONT-END AC–DC CONVERTER TOPOLOGIES

As a key component of a charger system, the front-end AC–DC converter must achieve high efficiency and high power density. Additionally, to meet the efficiency and power factor requirements and regulatory standards for the AC supply mains, PFC is essential.

As the adoption rate of these vehicles increases, the stress on the utility grid is projected to increase significantly at times of peak demand. Therefore, efficient and high power factor charging is critical in order to minimize the utility load stress, and reduce the charging time. In addition, a high power factor is needed to limit the input current harmonics drawn by these chargers and to meet regulatory standards, such as IEC 1000-3-2 [4].

According to the requirements of input current harmonics and output voltage regulation, a front-end converter is normally implemented by a PFC stage. Conventionally, most of the power conversion equipment employs either a diode rectifier or a thyristor rectifier with a bulk capacitor to

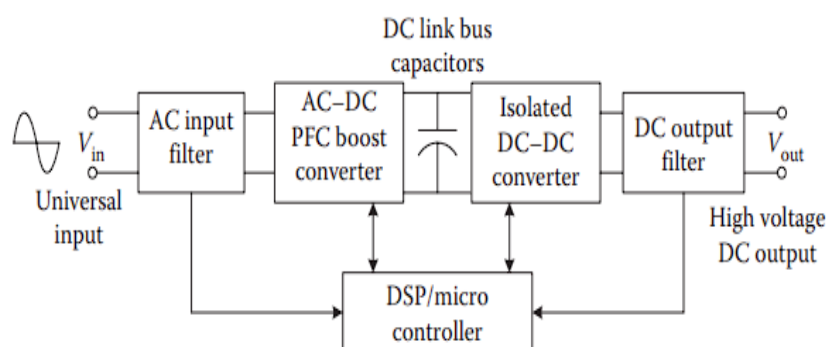


FIGURE 13.1 Simplified system block diagram of a universal on-board two-stage battery charger.

convert AC voltage to DC voltage before processing it. Such rectifiers produce input current with rich harmonic content, which pollute the power system and the utility lines. Power quality is becoming a major concern for many electrical users.

The simplest form of PFC is passive (passive PFC). A passive PFC uses a filter at the AC input to correct poor power factor. The passive PFC circuitry uses only passive components—an inductor and some capacitors. Although pleasantly simple and robust, a passive PFC rarely achieves low total harmonic distortion (THD). Furthermore, because the circuit operates at the low line power frequency of 50 or 60 Hz, the passive elements are normally bulky and heavy. Figure 13.2 shows input voltage and current for a passive PFC and the harmonic spectrum of input current.

The input power factor (PF) is defined as the ratio of the real power over apparent power as

$$\text{Power factor (PF)} = \frac{\text{Real power (W)}}{\text{Apparent power (VA)}} \quad (13.1)$$

Assuming an ideal sinusoidal input voltage source, the power factor can be expressed as the product of two factors, the distortion factor and the displacement factor, given as

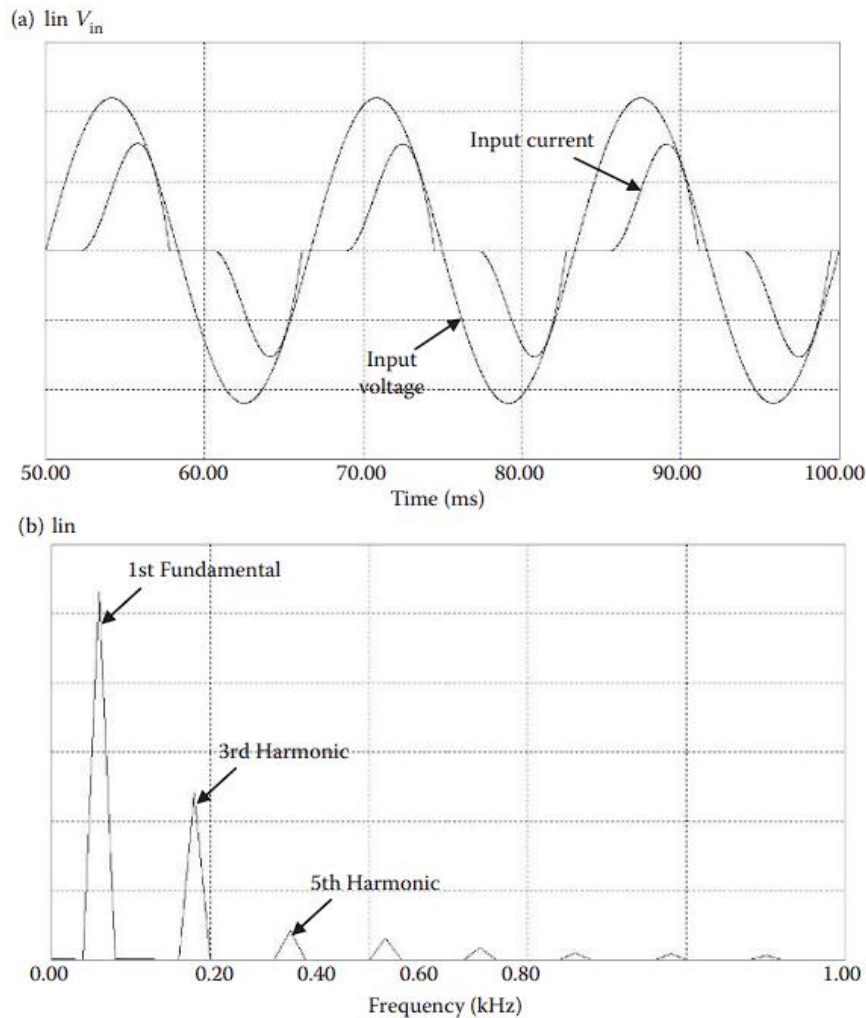


FIGURE 13.2 Passive power factor correction AC main voltage and current waveforms. (a) Input voltage and input current. (b) Harmonic spectrum of input current.

BEYOND SYLLABUS:

PM SYNCHRONOUS MOTOR DRIVES:

A typical PM synchronous motor drive consists of a PM synchronous motor, a three-phase bridge inverter, gate drivers, position sensor, current or voltage sensors, a microprocessor, and its interfacing circuits, as shown in Figure 8.19

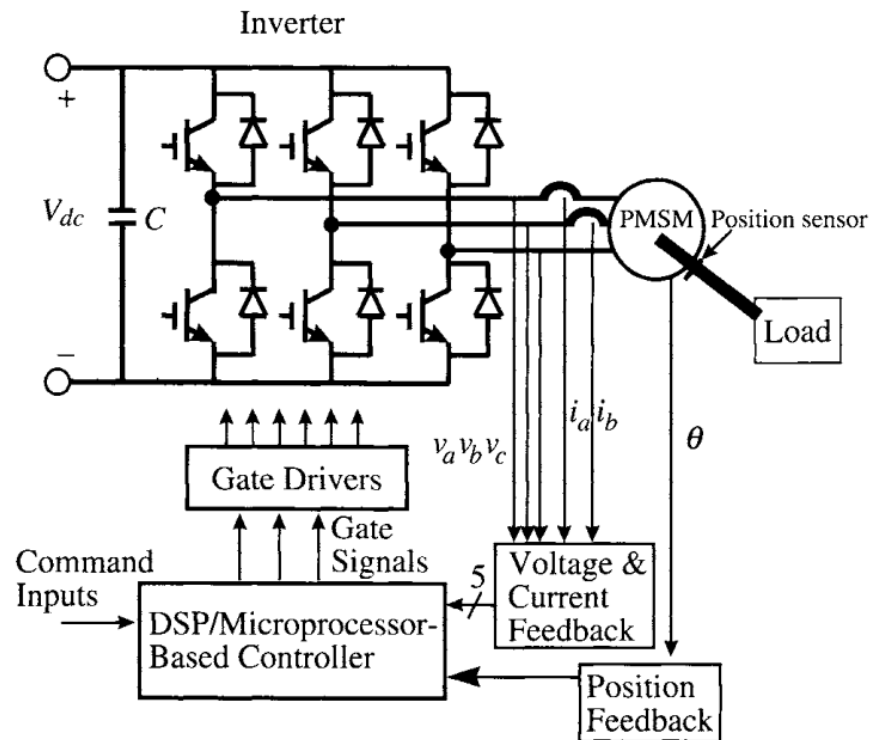


FIGURE 8.19 A typical PM synchronous motor drive structure.

system controller sets the reference or command signal, which can be position, speed, current, or torque. The variables needed for the controller are the feedback signals from the sensing circuits (position, speed, current, or voltage) or estimated values in the signal processor. The error signals between the reference and actual variable signals are transformed to gate control signals for the inverter switches. The switches follow the gate commands to decrease the error signals by injecting desired stator currents into the three-phase stator windings.

VECTOR CONTROL

Vector control is used for the PM synchronous motor drive in EV and HEV applications to deliver required performance. Torque Equation 6.2 for the PM synchronous motor shows that if the d -axis current is maintained constant, the generated torque is proportional to the q -axis current. For the special case when i_d is forced to be zero, $\lambda_d = \lambda_{af}$ and

$$\begin{aligned} T_e &= \frac{3}{2} \cdot \frac{P}{2} \cdot \lambda_{af} \cdot i_q \\ &= k_e i_q \end{aligned} \quad (8.28)$$

where

$$k_e = \frac{3}{2} \cdot \frac{P}{2} \cdot \lambda_{af}$$

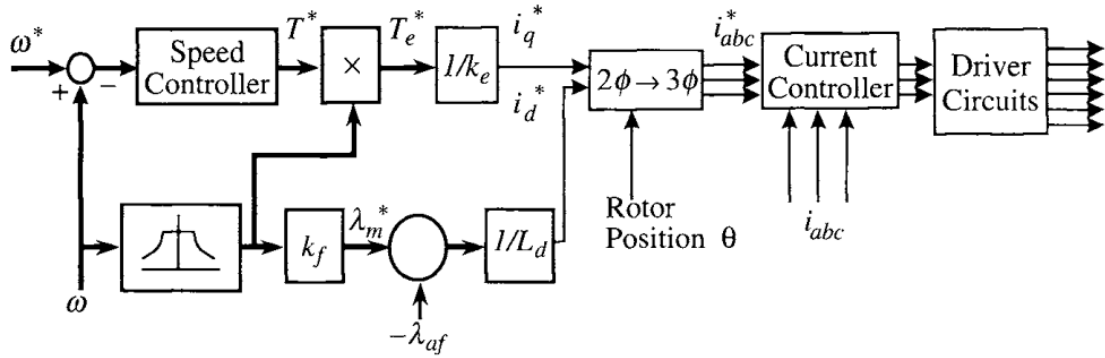


FIGURE 8.20 Vector controller structure for PMSM with field weakening.

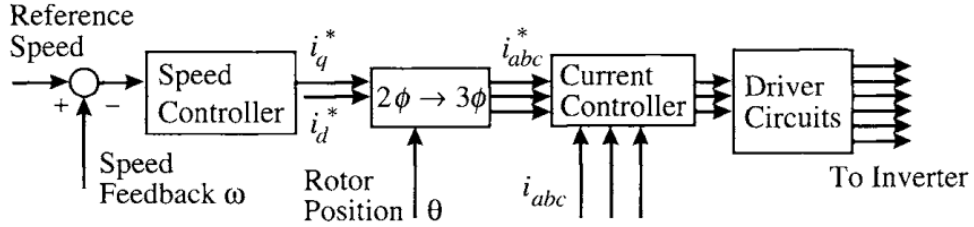


FIGURE 8.21 Current controller block diagram.

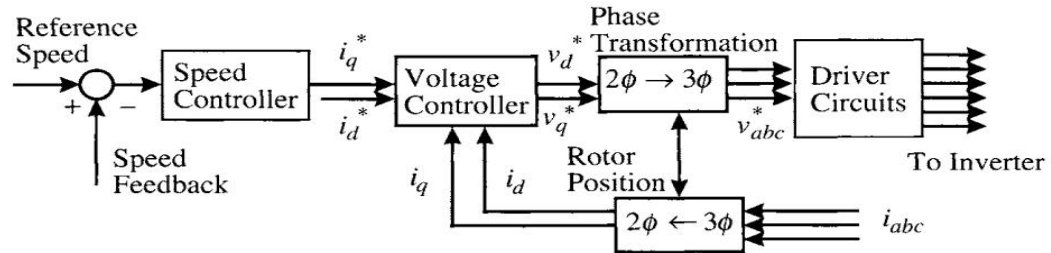


FIGURE 8.22 Voltage controller block diagram.

=motor constant. Because the magnetic flux linkage is a constant, torque is directly proportional to q -axis current. The torque equation is similar to that of a separately excited DC machine. Therefore, using reference frame transformations, the PM synchronous motor can be controlled like a DC machine.

8.4.1 SRM CONVERTERS

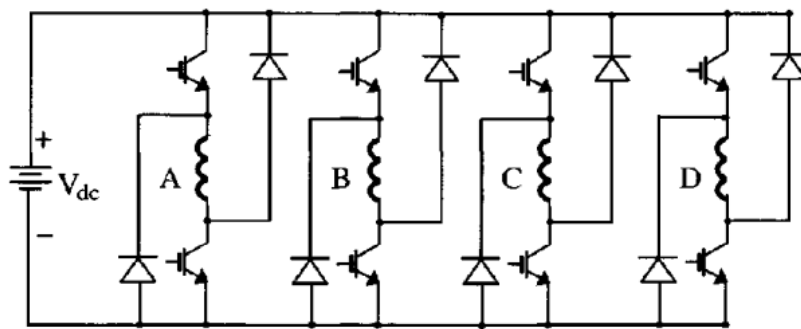
The most flexible and the most versatile four-quadrant SRM converter is the bridge converter, shown in Figure 8.23a, which requires two switches and two diodes per phase.^{7,8} The switches and the diodes must be rated to withstand the supply voltage plus any transient overload. During the magnetization period, both switches are turned on, and the energy is transferred from the source to the motor. Chopping or PWM, if necessary, can be accomplished by switching either or both of the switches during the conduction period, according to the control strategy. At commutation, both switches are turned off, and the motor phase is quickly defluxed through the freewheeling diodes. The main advantage of this converter is the independent control of each phase, which is particularly important when phase overlap is desired. The only disadvantage is the requirement of two switches and two diodes per phase. This converter is especially suitable for high-voltage, high-power drives.

The split-capacitor converter shown in Figure 8.23b has only one switch per phase but requires a split DC supply.⁷ The phases are energized through the upper or the lower DC bus rail and the midpoint of the two capacitors. Therefore, only one-half the DC bus voltage can be applied for torque production. In order to maintain power flow balance between the two supply capacitors, the switching device and the freewheeling diode are transposed for each phase winding, which means that the motor must have an even number of phases. Also, the power devices must be rated to withstand the full DC supply voltage.

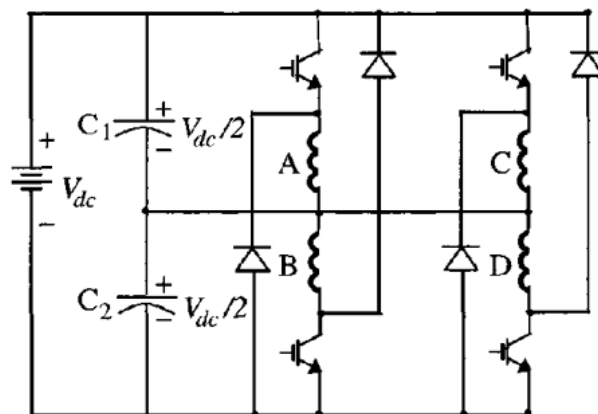
In low-speed applications, where PWM current control is desirable over the entire range of operation, the bridge converter can be reduced to the circuit shown in Figure 8.23c, developed by Miller.⁸ In this converter, chopping is performed by one switch common to all phases. The circuit requires $(n+1)$ switches for an n -phase motor. The main limitation of this circuit is that at higher speeds, the off-going phase cannot be de-energized fast enough, because the control switch Q1 keeps turning on intermittently, disabling forced demagnetization. A class of power converter circuits with less than two switches per phase for SR motors having four or more phases has been developed by Pollock and Williams.⁹

The energy-efficient C-dump converter shown in Figure 8.23d is a regenerative converter topology with a reduced number of switches.¹⁰ The topologies were derived from the C-dump converter proposed earlier by Miller.⁸ The energy-efficient converter topologies eliminate all the disadvantages of the C-dump converter without sacrificing its attractive features, and they also provide additional advantages. The attractive features of the converters include a lower number of power devices, full regenerative capability, freewheeling in chopping or PWM mode, simple control strategy, and faster demagnetization during commutation. The energy-efficient C-dump converter has one switch plus one diode forward voltage drop in the phase magnetization paths.

Converters with a reduced number of switches are typically less fault-tolerant compared to the bridge converter. The ability to survive component or motor phase failure should be a prime consideration for high-reliability applications. On the other hand, in low-voltage applications, the voltage drop in two switches can be a significant percentage of the total bus voltage, which may not be affordable. Among other factors to be considered in selecting a drive circuit are cost, complexity in control, number of passive components, number of floating drivers required, etc. The drive converter must be chosen to serve the particular needs of an application.



(a)



(b)

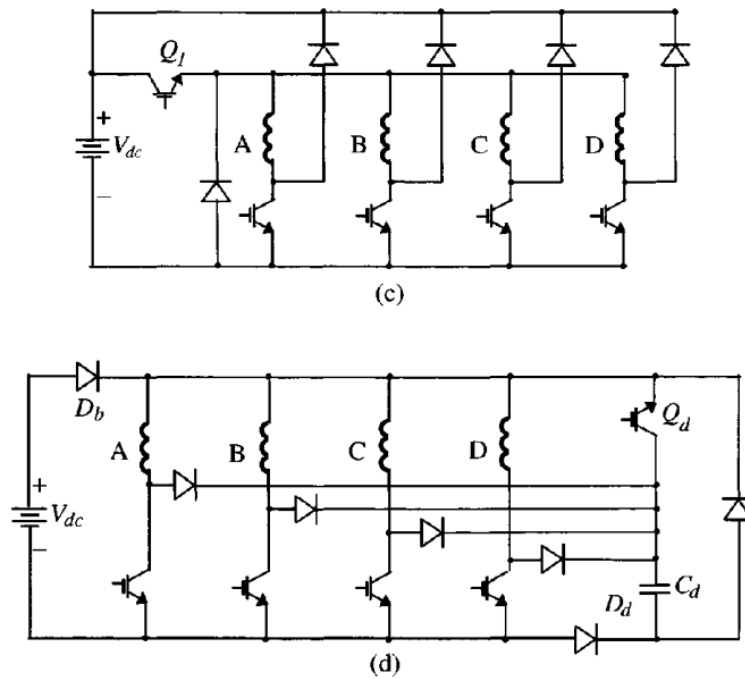


FIGURE 8.23 Converter topologies for SRM: (a) classic bridge power converter; (b) split-capacitor converter; (c) Miller converter; and (d) energy-efficient converter.

SRM CONTROLS:

Voltage-Controlled Drive

In low-performance drives, where precise torque control is not a critical issue, fixed-frequency PWM voltage control with variable duty cycle provides the simplest means of control of the SRM drive. A highly efficient variable speed drive having a wide speed range can be achieved with this motor by optimum use of the simple voltage feeding mode with closed-loop position control only. The block diagram of the voltage-controlled drive is shown in [Figure 8.24](#). The angle controller generates the turn-on and turn-off angles for a phase, depending on the rotor speed, which simultaneously determines the conduction period, θ_{dwell} . The duty cycle is adjusted according to the voltage command signal. The electronic commutator generates the gating signals based on the control inputs and the instantaneous rotor position. A speed feedback loop can be added on the outside, as shown when precision speed control is desired. The drive usually incorporates a current sensor typically placed on the lower leg of the DC link for overcurrent protection. A current feedback loop can also be added that will further modulate the duty cycle and compound the torque-speed characteristics, just like the armature voltage control of a DC motor.

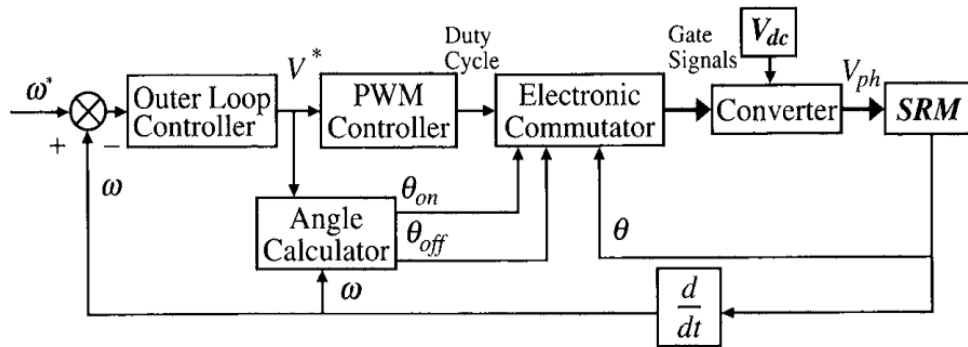


FIGURE 8.24 Voltage-controlled drive.

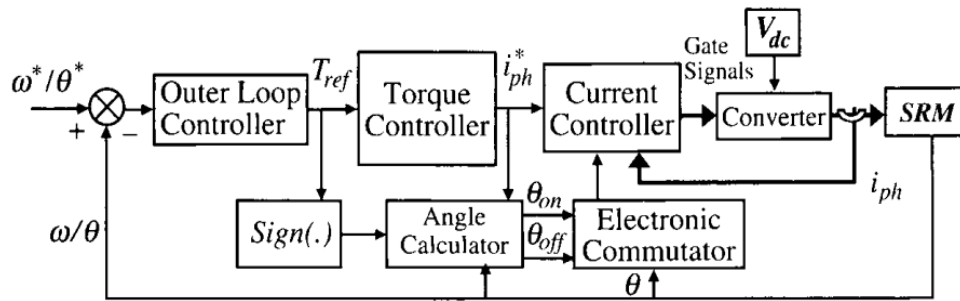


FIGURE 8.25 Current-controlled drive.

Current-Controlled Drive

In torque-controlled drives, such as in high-performance servo applications, the torque command is executed by regulating the current in the inner loop, as shown in Figure 8.25. The reference current i^* for a given operating point is determined from the load characteristics, the speed, and the control strategy. A wide-bandwidth current transducer provides the current feedback information to the controller from each of the motor phases. This mode of control allows rapid resetting of the current level and is used where fast motor response is desired. For loads with torque that increases monotonically with speed, such as in fans or blowers, speed feedback can be introduced in the outer loop for accurate speed control.

The simpler control strategy is to generate one current command to be used by all the phases in succession. The electronic commutator (see Figure 8.25) selects the appropriate phase for current regulation based on θ_{on} , θ_{off} , and the instantaneous rotor position. The current controller generates the gating signal for the phases based on the information coming from the electronic commutator. The current in the commutated phase is quickly brought down to zero, applying negative V_{dc} , while the incoming phase assumes the responsibility of torque production based on the commanded current. The phase transition in these drives is not smooth, which tends to increase the torque ripple of the drive.